Magnetoviscosity in dilute ferrofluids from rotational Brownian dynamics simulations

D. Soto-Aquino and C. Rinaldi*

Department of Chemical Engineering, University of Puerto Rico, Mayagüez Campus, P.O. Box 9000, Mayagüez 00681, Puerto Rico

(Received 18 May 2010; published 22 October 2010)

Ferrofluids are suspensions of magnetic nanoparticles which respond to imposed magnetic fields by changing their viscosity without losing their fluidity. Prior work on modeling the behavior of ferrofluids has focused on using phenomenological suspension-scale continuum equations. A disadvantage of this approach is the controversy surrounding the equation describing the rate of change of the ferrofluid magnetization, the so-called magnetization relaxation equation. In this contribution the viscosity of dilute suspensions of spherical magnetic nanoparticles suspended in a Newtonian fluid and under applied shear and constant magnetic fields is studied through rotational Brownian dynamics simulations. Simulation results are compared with the predictions of suspension-scale models based on three magnetization relaxation equations. Excellent agreement is observed between simulation results and the predictions of an equation due to Martsenyuk, Raikher, and Shliomis. Good qualitative agreement is observed with predictions of other equations, although these models fail to accurately predict the magnitude and shear rate dependence of the magnetic-field-dependent effective viscosity. Finally, simulation results over a wide range of conditions are collapsed into master curves using a Mason number defined based on the balance of hydrodynamic and magnetic torques.

DOI: 10.1103/PhysRevE.82.046310 PACS number(s): 47.57.Qk, 47.65.Cb

I. INTRODUCTION

Ferrofluids are colloidal suspensions of magnetic nanoparticles that exhibit normal liquid behavior in the absence of magnetic fields, but respond to imposed magnetic fields by changing their viscosity without loss of fluidity. In a suspension of magnetic particles with particle-locked magnetic dipole moments under the influence of a shear flow field the particles will rotate with their axes of rotation parallel to the vorticity of the flow [1]. As long as there is no external magnetic field and the particle concentration is not too high, the properties of the suspension are close to the properties of the suspending liquid, and the viscosity satisfies the formula obtained by Einstein [2]

$$\eta = \eta_0\left(1 + \tfrac{5}{2}\tilde{\phi}\right). \qquad (1)$$

Here η_0 stands for the viscosity of the carrier liquid, η stands for the viscosity of the suspension in the absence of a magnetic field, and $\tilde{\phi}$ denotes the volume fraction of all suspended materials. If a magnetic field is applied to the suspension the particles will rotate relative to the fluid resulting in a change in viscosity, and the Einstein result is no longer applicable. The increase in viscosity due to the magnetic field is often termed the rotational viscosity or magnetoviscosity of the fluid.

The first experimental report of changes in viscosity due to a magnetic field was published by Rosensweig *et al.* in 1969 [3], who carried out experiments over a wide range of variables such as solvent viscosity, ferric induction, particle diameter, temperature, applied field, shear rate, and number concentration. They observed viscosity increments in ferrofluids under shear and magnetic fields. The viscosity of the fluid in a magnetic field was also estimated by dimensional analysis and verified experimentally. Subsequently McTague [4] described the magnetoviscosity of a highly dilute colloidal suspension of cobalt particles in a Hagen-Poiseuille flow.

Suspension-scale models to describe the effect of magnetic fields on the viscosity of ferrofluids have been developed by Shliomis (Sh) [5,6], Martsenyuk *et al.* [7], Felderhof [8], and others [9,10]. These models often differ in the assumptions made for the so-called magnetization relaxation equation [5–8,10,11], underscoring the controversy found in the macroscopic description of ferrofluid flow, even in the infinitely dilute limit. The most commonly used magnetization equation was developed by Shliomis in 1972 [5]. Shliomis' analysis stems from the use of a macroscopic *ad hoc* phenomenological magnetization equation obtained as a modification of the Debye relaxation equation and is given by

$$\frac{d\mathbf{M}}{dt} = \mathbf{\Omega} \times \mathbf{M} - \frac{1}{\tau}(\mathbf{M} - \mathbf{M}_0) - \frac{1}{6\eta\phi}\mathbf{M} \times (\mathbf{M} \times \mathbf{H}). \qquad (2)$$

Here, $\mathbf{M}$ stands for the ferrofluid magnetization under the magnetic field $\mathbf{H}$ and the flow vorticity $\mathbf{\Omega} = \frac{1}{2}\nabla \times \mathbf{v}$. In Eq. (2) $\tau_B = 3\eta V/k_B T$ stands for the characteristic Brownian relaxation time of rotational particle diffusion, since the particles are assumed to possess particle-locked magnetic dipoles. At equilibrium in a stationary field, $\mathbf{M}_0$ is described well by the Langevin function

$$\mathbf{M_0} = nmL(\alpha)\frac{\mathbf{H}}{H}, \quad \alpha = \frac{mH}{k_B T}, \quad L(\alpha) = \coth \alpha - \alpha^{-1}, \qquad (3)$$

where m is the magnetic dipole moment of a single particle, n is the number density of the particles, and α is the Langevin parameter. Considering rotational motion of the particles relative to the carrier liquid and Eq. (3), Shliomis derived an equation for the rotational viscosity in a planar Poiseuille or

*Author to whom correspondence should be addressed; carlos.rinaldi@upr.edu

Couette flow under the influence of a constant uniform magnetic field. The result is

$$\eta_r = \tfrac{1}{4}\tau_\perp M_0 H, \tag{4}$$

where $\tau_\perp = 2\tau_B/[2+\alpha L(\alpha)]$ is the relaxation time of the transverse (to the field) component of the magnetization. According to Shliomis [5], in the limit of low shear rate and short magnetization relaxation time, $\Omega\tau_B \ll 1$, the rotational viscosity is given by

$$\eta_r(\alpha) = \frac{3}{2}\phi\eta_0 \frac{\alpha - \tanh\alpha}{\alpha + \tanh\alpha}\sin^2\beta, \tag{5}$$

where β is the angle between field and vorticity.

Shortly thereafter, Martsenyuk, Raikher, and Shliomis (MRSh) [7] proposed another magnetization equation derived microscopically from the Fokker-Planck equation. They employed for this purpose an effective-field method which results in closure of the first moment of magnetization. The MRSh magnetization equation is then

$$\frac{d\mathbf{M}}{dt} = \mathbf{\Omega}\times\mathbf{M} - \frac{\mathbf{H}[\mathbf{H}\cdot(\mathbf{M}-\mathbf{M}_0)]}{\tau_\parallel H^2} - \frac{\mathbf{H}\times(\mathbf{M}\times\mathbf{H})}{\tau_\perp H^2}, \tag{6}$$

where $\tau_\parallel = d\ln L(\alpha)/d\ln\alpha$ and $\tau_\perp = \{2L(\alpha)/[\alpha - L(\alpha)]\}\tau$ are the parallel and transverse relaxation times. Using Shliomis' definition for the rotational viscosity [Eq. (4)], Martsenyuk *et al.* [7] obtained for the rotational viscosity

$$\eta_r(\alpha) = \frac{3}{2}\eta\phi\frac{\alpha L^2(\alpha)}{\alpha - L(\alpha)}. \tag{7}$$

Tsebers [12] compared the Sh′72 and MRSh equations using numerical simulations of the Brownian motion of ferromagnetic particles to study the field dependence of the magnetization relaxation time. These simulations indicated that the MRSh equation provides an excellent description of the dynamics of fluid magnetization in the absence of shear. Although this work was an important step in evaluating these equations, further work is needed to understand the effect of shear and compare predictions for the magnetoviscosity for both equations.

Several years later Shliomis [6] proposed yet another magnetization equation derived from irreversible thermodynamics and employed it in the calculation of the rotational viscosity in a magnetic field. This third magnetization equation is

$$\frac{d\mathbf{H}_e}{dt} = \mathbf{\Omega}\times\mathbf{H}_e - \frac{1}{\tau}(\mathbf{H}_e - \mathbf{H}) - \frac{1}{6\eta\phi}\mathbf{H}_e\times(\mathbf{M}\times\mathbf{H}). \tag{8}$$

In Eq. (10) the effective field $\mathbf{H}_e$ is that corresponding to the nonequilibrium magnetization, obtained from the inverse Langevin function. For low field strength, Eq. (8) predicts the same dependence, described by Eq. (5), of rotational viscosity on the magnetic field strength as Eq. (2).

It will be seen in the simulations discussed below that the shear rate $\dot{\gamma}$, parametrized through the rotational Péclet number $\mathrm{Pe}_r = \dot{\gamma}/D_r$, where D_r is the rotational diffusivity of the magnetic particles, has a significant effect on the magnetoviscosity. Hence, it is important to know the predictions of the above mentioned relaxation equations for the shear rate dependence of the magnetoviscosity. In order to obtain the shear rate dependence of the rotational viscosity predicted by the various magnetization equations, it is convenient to pass from the fields $\mathbf{H}$ and $\mathbf{H}_e$ to their nondimensional values of α and ε. According to Shliomis [6], both Eqs. (2) and (8) admit a steady solution in which the effective field tracks the true field with lag angle γ. The dependence of the effective field, ε and γ, and true field α on $\Omega\tau$ for Eq. (2) is given by

$$\sqrt{\alpha^2 - \varepsilon^2} = \frac{2\Omega\tau\alpha\varepsilon}{2\alpha + \varepsilon^2 L(\varepsilon)}, \quad \cos\gamma = \frac{\varepsilon}{\alpha}. \tag{9}$$

Taking into consideration Eqs. (4) and (9), the rotational viscosity is then

$$\eta_r = \frac{3}{2}\eta\phi\frac{\varepsilon^2 L(\alpha)}{2\alpha + \varepsilon^2 L(\varepsilon)}. \tag{10}$$

Similarly for the MRSh equation [Eq. (6)], the effective field ε and field α are related by

$$\sqrt{\alpha^2 - \varepsilon^2} = \frac{2\Omega\tau\varepsilon L(\varepsilon)}{\varepsilon - L(\varepsilon)}, \quad \cos\gamma = \frac{\varepsilon}{\alpha}, \tag{11}$$

which results in the following expression for the rotational viscosity:

$$\eta_r = \frac{3}{2}\eta\phi\frac{\varepsilon L^2(\varepsilon)}{\varepsilon - L(\varepsilon)}. \tag{12}$$

Finally, for the third relaxation equation [Eq. (8)], the effective field ε and field α are related by

$$\sqrt{\alpha^2 - \varepsilon^2} = \frac{2\Omega\tau\varepsilon}{2 + \varepsilon L(\varepsilon)}, \quad \cos\gamma = \frac{\varepsilon}{\alpha}, \tag{13}$$

which results in

$$\eta_r = \frac{3}{2}\eta\phi\frac{\varepsilon L(\varepsilon)}{2 + \varepsilon L(\varepsilon)}. \tag{14}$$

Several researchers [13–17] have experimentally investigated the rheological properties of ferrofluids using rotational rheometers. Most of these studies compared experimental results with theoretical models of the magnetic viscosity [17–20]. For example, Patel *et al.* [21] compared the viscosity of a magnetic fluid obtained experimentally with the MRSh and Felderhof [8] magnetoviscosity expressions. However, in contrast with most analyses, in the work of Patel *et al.* the magnetic field was applied perpendicular to the axis of the capillary viscometer; hence, the direction of the field was not uniformly perpendicular to the vorticity of the flow. In analyzing their data, Patel *et al.* assumed that the magnetoviscosity depends on the angle β between the vorticity and magnetic field according to Eq. (5), which is with a correction factor of $\sin^2\beta$, and used this correction factor to compare the predictions of Sh′72, MRSh, and Felderhof to their measurements using a capillary tube. Note that although the $\sin^2\beta$ dependence in Eq. (5) for the Sh′72 magnetization relaxation equation was derived analytically, this result is only applicable for small fields and shear rates, and the predicted $\sin^2 \beta$ is not necessarily applicable for the other equations tested by Patel *et al.* Whether this assumed dependence is correct is subject to further inquiry and is discussed below.

Because ferrofluids are opaque, measurement of bulk flow profiles is challenging [22,23]. On the other hand, there are no methods to measure the average rate of spin of the particles (the so-called spin velocity). In addition, it is not always possible to orient the direction of the applied field uniformly in a direction that is perpendicular or parallel to the vorticity of the flow. Also, most ferrofluids used in experiments contain high particle concentrations, resulting in particle-particle magnetic interactions such as chaining, the effects of which are not captured by the preceding theories. Finally, because most ferrofluids consist of nanoparticles suspended in low-viscosity carrier fluids, the shear rates typically obtained in experiments are not sufficient to explore the full shear rate dependence predicted by theory. The preceding experimental limitations make direct particle-scale simulations an attractive tool to improve the understanding of the macroscopic behavior of dilute ferrofluids, to explore the applicability and limitations of suspension-scale governing and constitutive equations, and to develop new applications.

The rheological properties of ferrofluids have been studied by numerical simulations such as in the work of Morimoto *et al.* [24], who studied the so-called negative viscosity effect predicted theoretically by Shliomis and Morozov [25]. Morimoto *et al.* studied this effect in a two-dimensional magnetic fluid composed of disklike particles subjected to shear flow and alternating magnetic fields. They found that the rotational viscosity is high when the frequency of the magnetic field is low, and it becomes negative in an intermediate frequency range. Satoh and Ozaki studied the influence of the magnetic field strength, shear rate, and rotational Brownian motion on transport coefficients such as viscosity and diffusivity in dilute suspensions of rodlike [26] and spherocylinder [27] particles. The results in both cases show that the orientation distribution is dependent on the relative ratio of magnetic field and shear rate. Sánchez and Rinaldi [28] used rotational Brownian dynamics simulations to study the rheological properties of ellipsoidal particles in magnetic and shear flow fields. They found that ellipsoidal particles show a significant effect of aspect ratio on the intrinsic magnetoviscosity of the suspension. In addition, they also found that it is possible to fit the data for ellipsoids to a master curve by defining an effective Péclet number $\mathrm{Pe}_{r,eff} = \mathrm{Pe}_r(D_{r,\max}/D_{r,eff})$, where $D_{r,eff}$ is obtained from averaging the rotational diffusion tensor $\boldsymbol{D}_r'$ around the magnetic axis of the particle. More recently, Sánchez and Rinaldi [29] used Brownian dynamics simulations to study the effect of alternating and rotating magnetic fields on the viscosity of magnetic nanoparticle suspensions. These simulations demonstrated that the so-called negative viscosity effect is more pronounced under the application of rotating magnetic fields when the field corotates with the vorticity of the flow.

The purpose of this contribution is to offer additional insight into ferrohydrodynamics and the validity of the various magnetization relaxation equations in describing the so-called magnetoviscosity. In the present work we study the intrinsic magnetoviscosity of a magnetic fluid composed of noninteracting spherical permanently magnetized particles and subjected to a magnetic field and shear flow by Brownian dynamics simulations and compare the results with predictions of continuum level models. We also study the effect of the angle between the magnetic field and the vorticity on the magnetoviscosity. Finally, simulation results over a wide range of conditions are collapsed into master curves, which provide insight into the scaling laws relating magnetoviscosity, magnetic field strength, and shear rate, introducing a rotational Mason number. In Sec. II we introduce our model and magnetoviscosity calculation, in Sec. III we discuss the results obtained, and in Sec. IV we present our concluding remarks.

II. ROTATIONAL BROWNIAN DYNAMICS SIMULATIONS

A. Algorithm formulation

Rotational Brownian dynamics simulations are based on the integration of the stochastic angular momentum equation in a way to obtain the orientation of each particle. There are three kinds of torques acting on the particle: $\mathbf{T}_h$ due to hydrodynamic effects, $\mathbf{T}_m$ due to magnetic effects, and $\mathbf{T}_B$ due to Brownian motion. Because inertia is negligible for the usual particle size in ferrofluids, the torque balance that governs the rotational motion of the particles is

$$\mathbf{T}_h' + \mathbf{T}_m' + \mathbf{T}_b' = \mathbf{0}. \tag{15}$$

Here, the prime indicates a vector with respect to particle-locked coordinates. The torque due to hydrodynamic effects is given by

$$\mathbf{T}_h' = -\eta_0[K_r(\boldsymbol{\omega}' - 1/2\,\boldsymbol{\nabla}\times\mathbf{v}')]. \tag{16}$$

Here, η_0 is the viscosity of the fluid carrier, $K_r = 8\pi r^3$ the hydrodynamic rotational resistance coefficient, and $\boldsymbol{\omega}'$ and $1/2\boldsymbol{\nabla}\times\mathbf{v}'$ are the angular velocities of the particle and the fluid, respectively. The magnetic torque is given by

$$\mathbf{T}_m' = \mu_0(\mathbf{m}'\times\mathbf{H}'), \tag{17}$$

where μ_0 is the permeability of free space and $\mathbf{H}' = \mathbf{A}\cdot\mathbf{H}$ is the applied magnetic field, transformed to the body fixed axis using the transformation matrix $\mathbf{A}$, which is related to the Euler parameters by [30]

$$\mathbf{A} = \begin{bmatrix} e_0^2+e_1^2-e_2^2-e_3^2 & 2(e_1e_2+e_0e_3) & 2(e_1e_3+e_0e_2) \\ 2(e_1e_2-e_0e_3) & e_0^2-e_1^2+e_2^2-e_3^2 & 2(e_3e_2+e_0e_1) \\ 2(e_1e_3+e_0e_2) & 2(e_3e_2-e_0e_1) & e_0^2-e_1^2-e_2^2-e_3^2 \end{bmatrix}. \tag{18}$$

In order to reduce the number of variables in the angular momentum equation, time was nondimensionalized with respect to the rotational diffusion coefficient $D_r = k_BT(\eta_0K_r)^{-1}$, and the vector variables were nondimensionalized with respect to their corresponding magnitudes, as explained in prior work [28]. Setting $d\tilde{\boldsymbol{\Phi}}' = \tilde{\boldsymbol{\omega}}' d\tilde{t}$, where $d\tilde{\boldsymbol{\Phi}}'$ is the infinitesimal rotation vector, integrating from time $\tilde{t}$ to $\tilde{t}+\Delta\tilde{t}$ using a first-order forward Euler method, and applying the fluctuation-dissipation theorem to the Brownian term [31], we obtain

$$\Delta\tilde{\mathbf{\Phi}}' = \alpha(\tilde{\boldsymbol{\mu}}' \times \tilde{\mathbf{H}}')\Delta\tilde{t} - \mathrm{Pe}_r\, \tilde{\boldsymbol{\omega}}_f' \Delta\tilde{t} + \tilde{\mathbf{w}}'. \qquad (19)$$

The vector $\mathbf{w}'$ is a random vector which follows a Gaussian distribution with mean and covariance given by

$$\langle \tilde{\mathbf{w}}_i' \rangle = 0, \quad \langle \tilde{\mathbf{w}}_i' \tilde{\mathbf{w}}_i' \rangle = \mathbf{I}\Delta\tilde{t}. \qquad (20)$$

The algorithm proceeds from a starting configuration by calculating the change in orientation at each time step. After each time step the quaternion parameters of each particle are normalized. All runs were performed starting from a random configuration, using 10^5 noninteracting particles, a time step of $\Delta\tilde{t}=0.01$, Langevin parameters of $0.1<\alpha<100$, and dimensionless shear rates of $0.1<\mathrm{Pe}_r<100$. Angles between the magnetic field and vorticity varied between $0<\beta<\pi/2$.

B. Magnetoviscosity Calculation

In our simulations the magnetic dipole moment of the particle $\boldsymbol{\mu}'$ is directed along the z' axis, the simple shear flow is along the y axis, and the magnetic field $\mathbf{H}$ may have components along the x and z axes, according to the prescribed angle between field and vorticity. If the shear rate is denoted by $\dot{\gamma}$, then the unperturbed flow velocity $\mathbf{v}$ and the vorticity of the fluid $\boldsymbol{\omega}_f$ are given by

$$\mathbf{v} = \dot{\gamma} z \mathbf{i}_y, \quad \boldsymbol{\omega}_f = -\tfrac{1}{2}\dot{\gamma}\mathbf{i}_x. \qquad (21)$$

The apparent viscosity of the suspension due to the antisymmetric part of the viscous stress tensor is given by $\eta_{zy}^m = \tau_{zy}^m / \dot{\gamma}$, which is referred to as the magnetoviscosity of the suspension. For a dilute suspension, the intrinsic magnetoviscosity $[\eta_{zy}^m]$ is defined as

$$[\eta_{zy}^m] = \lim_{\phi\to 0} \frac{\eta_{zy}^m}{\phi \eta_0}. \qquad (22)$$

Using the transformation matrix the magnetoviscosity equation is expressed in terms of the quaternion parameters. The resulting equation is

$$[\eta_{zy}^m] = -3\frac{\alpha}{\mathrm{Pe}_r}\langle 2(e_2 e_3 - e_0 e_1)\tilde{H}_z \rangle_{zy}, \qquad (23)$$

regardless of the angle between the magnetic field and vorticity.

III. RESULTS

A. Comparison with continuum level models

Figure 1 shows the intrinsic magnetoviscosity of a suspension of spherical particles as a function of the Langevin parameter α and for different values of the rotational Péclet number [32]. At high values of α the intrinsic magnetoviscosity approaches a saturation value, indicating that the magnetic dipole moments of the particles are aligned with the magnetic field due to the preponderance of the magnetic torque over the Brownian and hydrodynamic torques. Moreover, the simulations do not predict a hysteresis of the magnetoviscosity at high shear and high field as calculated by Shliomis [5] and He *et al.* [33] using the ferrohydrodynamics

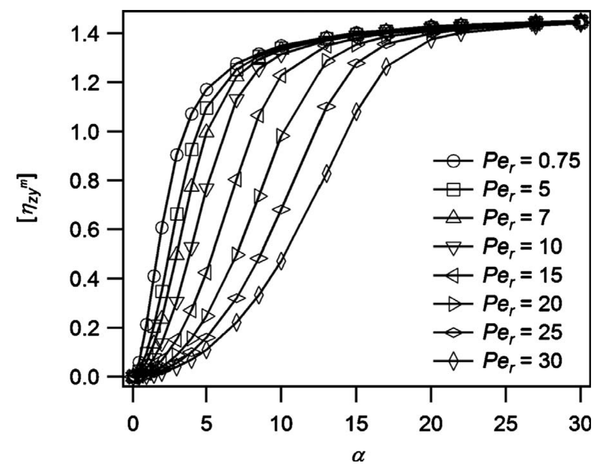

FIG. 1. Intrinsic magnetoviscosity of an infinitely dilute suspension of spherical particles with embedded dipoles as a function of the dimensionless magnetic field magnitude α, for different values of the dimensionless shear rate Pe_r.

equations and the Sh′72 magnetization relaxation equation.

Now we proceed to comparing the predictions for the magnetoviscosity of the various magnetization relaxation equations to the results of our simulations. In the case of $\mathrm{Pe}_r \ll 4$, corresponding to $\Omega\tau \ll 1$ in Shliomis and MRSh's analyses ($\Omega\tau=\mathrm{Pe}_r/4$), Eq. (7), obtained from the Sh′72 and Sh′01 equations, agrees with results obtained from our simulations at low and high α's but deviates from our results at intermediate values of α, as shown in Fig. 2. On the other hand, Eq. (9), obtained using the MRSh magnetization equation, is in excellent agreement with our results over the whole range of α, which indicates that the introduction of the concept of an effective field is a good approximation to the behavior of dilute ferrofluids.

When the ferrofluid is subjected to a sufficiently large shear rate, $\Omega\tau \geq 1$, the flow induces demagnetization since the magnetic particles tend to be rotated out of alignment with the magnetic field. Formally, this effect results in decreasing the parameter ε determined by Eqs. (11), (13), and (15).

Results for different values of $\Omega\tau$ for the Sh′72 equation [Eq. (12)], the MRSh equation [Eq. (14)], and the Sh′01 equation [Eq. (16)] are also shown in Fig. 2, compared with our simulation results. As seen from the figure, the higher the shear rate the larger the discrepancy between viscosity values predicted by the Sh′72 and Sh′01 equations and our results. On the other hand, the MRSh equation is in excellent agreement with our results under all conditions tested.

One might argue that for the commonly used low-viscosity ferrofluids it is difficult to achieve shear rates sufficient to see the effects of Fig. 2; however, this is not always the case. High-viscosity ferrofluids can be prepared for which the shear rate range typically accessible in rheometers should be sufficient to see these effects. More importantly and practically, ferrofluids are applied in fluid bearings such as in hard drive shafts. In such applications very high shear rates can be experienced by the ferrofluid. For example, in the work of Miwa *et al.* [34] ferrofluids are subjected to

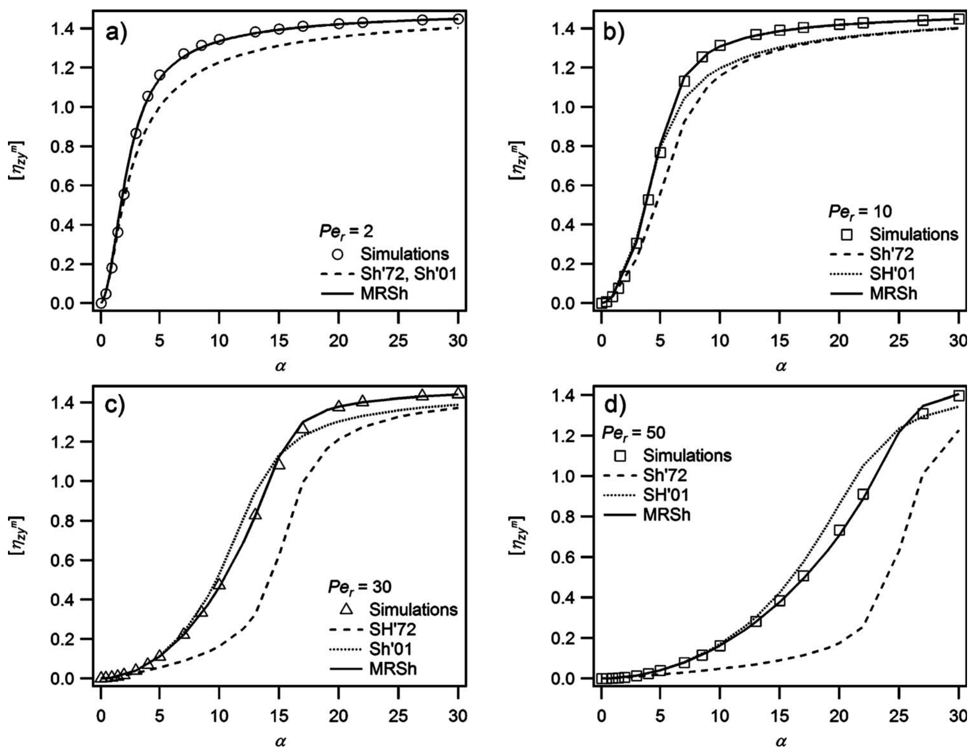

FIG. 2. Intrinsic magnetoviscosity as a function of the dimensionless magnetic field magnitude α, for different values of the dimensionless shear rate Pe_r, compared with the predictions of the Sh′72, Sh′01, and MRSh magnetization relaxation equations.

nominal shear rates as high as $10^8\ \mathrm{s}^{-1}$. For a typical ferrofluid with 10-nm-diameter nanoparticles and a base fluid viscosity of 10 cP this would correspond to a rotational Péclet number greater than 1000. Finally, the important point of the result of Fig. 2 is the demonstration that of the three magnetization relaxation equations being evaluated here, it is only the MRSh equation which yields results in quantitative agreement with direct simulations of the rotational dynamics of noninteracting Brownian magnetic nanoparticles over a wide range of values of the shear rate and magnetic field strength. Sh′72 and Sh′01 only yield results in qualitative agreement with the direct simulations. We note further that although the Sh′01 equation seems to be in better agreement with our simulations than the Sh′72 equation, the Sh′01 magnetization relaxation equation fails to correctly predict the relaxation dynamics of a ferrofluid from an applied equilibrium magnetic field, as shown in the Appendix.

Figure 3 shows the intrinsic magnetoviscosity of the suspension as a function of the magnetic field for different values of the angle β between the magnetic field and vorticity. Clearly, the factor $\sin^2\beta$ in Eq. (5) is not uniformly valid. This indicates, for example, that in the work of Patel *et al.* [21] the assumed relationship between the angle β and the magnetoviscosity is incorrect, except for very low or very high magnetic fields and shear rates. The fact that the often assumed $\sin^2\beta$ dependence of the magnetoviscosity on the angle β is incorrect has important implications for experiments aimed at determining the magnetic-field-dependent rheology of ferrofluids, as it indicates that experiments must be carried under conditions such that the vorticity and magnetic field are perpendicular throughout the sample. This constraint is particularly important if accurate determinations are desired under moderate magnetic fields and shear rates.

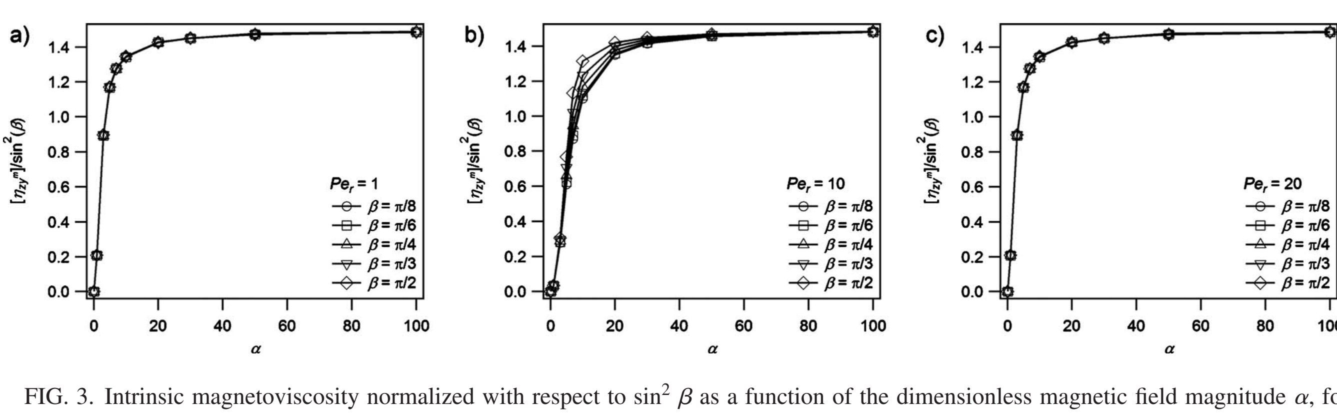

FIG. 3. Intrinsic magnetoviscosity normalized with respect to $\sin^2\beta$ as a function of the dimensionless magnetic field magnitude α, for different values of the dimensionless shear rate Pe_r and of the angle β between the magnetic field and vorticity.

B. Scaling of the magnetoviscosity using a Torque-based Mason number

As has been seen above, our direct simulations of the rotational dynamics of magnetic nanoparticles in shear and magnetic fields demonstrate that the continuum equations including the MRSh magnetization relaxation equation adequately describe the shear rate and magnetic field dependence of the magnetoviscosity of dilute ferrofluids. Another approach to the interpretation of the shear and magnetic field dependences of the viscosity of ferrofluids is the use of characteristic dimensionless parameters that capture the basic physics of the phenomena. In the closely related field of magnetorheological fluids, recent work has demonstrated that magnetorheological measurements over a wide range of conditions can be collapsed into master curves through the introduction of an appropriately defined Mason number [35]. This approach has also been adopted with respect to inverse ferrofluids [36] and magnetite-based ferrofluids [14,37]. In all these cases the working hypothesis is that the shear and magnetic field dependences of the viscosity of the suspension arise due to chain formation, with the magnetic field promoting chain formation and the shear field tending to destroy these chains. In these cases the particles are magnetizable; that is, their magnetic dipole moments are aligned with the local magnetic field and rotate freely within the particle. Chains form because of dipole-dipole interactions pulling particles together such that their dipoles align end to end. On the other hand, the shear field exerts a hydrodynamic force tending to pull the particles apart. On the basis of this balance of forces the Mason number is defined as

$$\mathrm{Mn} \equiv \frac{F_{\dot{\gamma}}}{F_H}, \tag{24}$$

where $F_{\dot{\gamma}}$ is the hydrodynamic force due to the shear and F_H is the magnetic force between dipoles. Using this definition of the Mason number the following expression is obtained [34,38,39]:

$$\mathrm{Mn} = \frac{\eta_0 \dot{\gamma}}{2\mu_0 \mu \beta^2 H_0^2}, \tag{25}$$

where $\beta = (\mu - \mu_0)/(\mu_0 + 2\mu) \approx 1$ is the magnetic contrast factor.

Although the Mason number defined according to Eqs. (24) and (25) has been appropriate for magnetorheological fluids and semidilute to concentrated ferrofluids composed of magnetic nanoparticles, it should be clear that it cannot be suitable to describe the magnetic field and shear dependences of the viscosity of infinitely dilute ferrofluids consisting of suspensions of nanoparticles with permanent magnetic dipoles (i.e., Brownian ferrofluids), for which Eqs. (5) and (7) apply. This is because in the infinitely dilute limit chains cannot form. However, as will be shown below, the magnetic field and shear dependences of the viscosity of these fluids can be adequately described using a Mason number defined as the ratio of hydrodynamic and magnetic torques on the particles.

For the following it will make more sense to recast the results shown in Fig. 1 as intrinsic magnetoviscosity as a function of dimensionless shear rate Pe_r. This is shown in Fig. 4, wherein it is seen that the intrinsic magnetoviscosity for low Pe_r has a plateau value which is a function of the magnetic field strength, parametrized by α. With increasing Pe_r the intrinsic magnetoviscosity is seen to decrease, that is, the fluid shear thins. It is seen that the critical Pe_r for shear thinning is a function of α; however, the curves for each α have similar shape, suggesting that an appropriate scale may exist that collapses the data. Here, we show how this can be done using a Mason number defined as the ratio of magnetic to hydrodynamic torques on the particles.

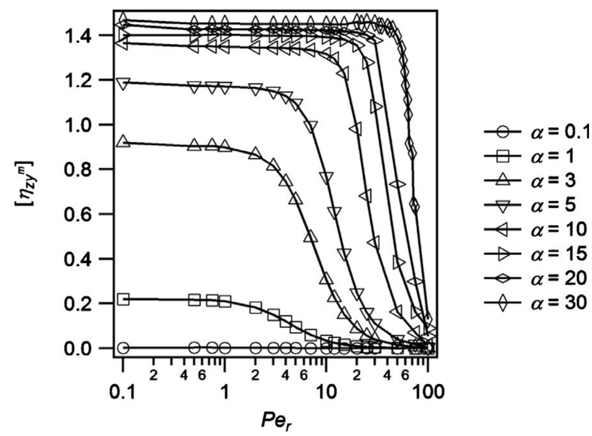

FIG. 4. Intrinsic magnetoviscosity of a suspension of spherical particles as a function of rotational Péclet number for different values of the Langevin parameter

Figure 5 illustrates the orientation distribution of the magnetic dipoles for a series of simulations at a constant value of the parameter α. The value of $\alpha = 30$ was chosen as this produces a shaper distribution around an average orientation. It is seen that as Pe_r increases from 0.1 to 60 the average orientation of the particles increases from an angle of almost 0 to close to 90 with respect to the direction of the magnetic field. This range of values of Pe_r correspond to the plateau

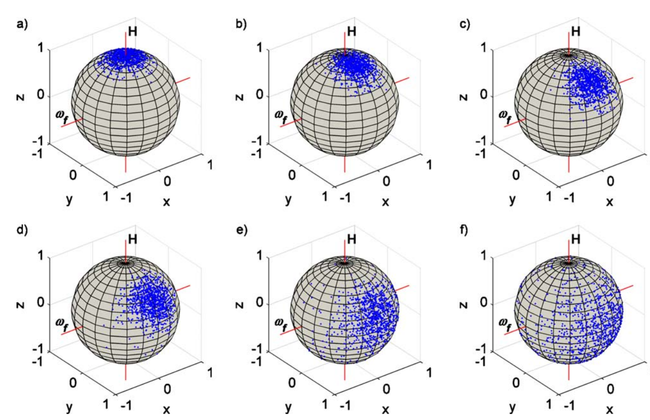

FIG. 5. (Color online) Orientation distributions of the magnetic dipole moments of the magnetic particles of (a) $\mathrm{Pe}_r = 1.0$, (b) $\mathrm{Pe}_r = 20.0$, (c) $\mathrm{Pe}_r = 40.0$, (d) $\mathrm{Pe}_r = 50.0$, (e) $\mathrm{Pe}_r = 60$, and (f) $\mathrm{Pe}_r = 75$ and $\alpha = 30.0$. Each dot corresponds to a particle with its magnetic dipole moment aligned with the corresponding point in the unit sphere. The directions of the magnetic field H and vorticity of the flow ω_f are shown.

region of the intrinsic magnetoviscosity for $\alpha=30$, shown in Fig. 4, and to the situation in which the dipoles do not, on average, rotate due to the balance of hydrodynamic and magnetic torques. On the other hand for $Pe_r > 60$ the particles begin to rotate as the hydrodynamic torque exceeds the magnetic torque. This range of values of the Péclet number correspond to the shear thinning region of the intrinsic magnetoviscosity for $\alpha=30$, shown in Fig. 4. These observations suggest that an angle of 90° between the average particle orientation and the magnetic field corresponds to the critical condition for which shear thinning occurs in the fluid.

As discussed above, the magnetic field and shear dependences of the viscosity of magnetorheological and chain-forming ferrofluids can be described using the so-called Mason number. Here, we obtain a Mason number based on the balance of hydrodynamic and magnetic torques on the particles. We proceed by recognizing that the source of the magnetoviscosity in an infinitely dilute suspension of Brownian nanoparticles is the hindered rotation arising from the tendency to align the particle's dipoles with the applied magnetic field. Such hindered rotation results in increased energy dissipation in the fluid surrounding the particles, and hence in an increased suspension-scale viscosity. The magnetic torque hindering the particle's rotation is opposed by the hydrodynamic torque exerted by the fluid on the particles. A shear-dependent decrease in the magnetoviscosity of the ferrofluid (shear thinning) is observed when the hydrodynamic torque exceeds the maximum magnetic torque on the particles, and hence the particles begin to rotate with the surrounding fluid. We define a torque-based Mason number Mn_T for this case as

$$Mn_T \equiv \frac{T_{\dot{\gamma}}}{T_H}, \tag{26}$$

where $T_{\dot{\gamma}}$ is the hydrodynamic torque exerted by the surrounding fluid on the particle, given by

$$T_{\dot{\gamma}} = 8\pi r^3 \eta_0 \frac{\dot{\gamma}}{2}, \tag{27}$$

and T_H is the maximum magnetic torque, corresponding to the condition when the particle's dipole is perpendicular to the applied magnetic field, given by

$$T_H = \mu_0 \mu H. \tag{28}$$

Substituting Eqs. (27) and (28) in Eq. (26) yields

$$Mn_T = \frac{8\pi r^3 \eta_0 \dot{\gamma}}{2\mu_0 \mu H} = \frac{Pe_r}{2\alpha}. \tag{29}$$

Comparing Eqs. (25) and (29) it is interesting that both depend on the relative magnitudes of the shear rate $\dot{\gamma}$ and magnetic field H. Both Mason numbers are linear in the shear rate; however, the force-based Mason number in Eq. (25) is proportional to the inverse square of the magnetic field, whereas the torque-based Mason number in Eq. (29) is proportional to the inverse of the magnetic field.

The results for the magnetoviscosity for all of our simulations in which the magnetic field and vorticity are perpendicular are plotted as functions of the torque-based Mason number in Fig. 6. For comparison purposes the predictions of the MRSh equation are shown as solid lines for selected values of Pe_r. It is evident from this figure that for each value of the dimensionless shear rate, Pe_r, the intrinsic magnetoviscosity is initially constant and equal to 3/2 and then decreases as a power law for high values of Mn_T, wherein $[\eta_{zy}^m] = A\ Mn_T^{-2}$, with A being a Pe_r-dependent proportionality factor. Note that for large values of Pe_r the results collapse into a single master curve, that is, A eventually asymptotes to a constant value.

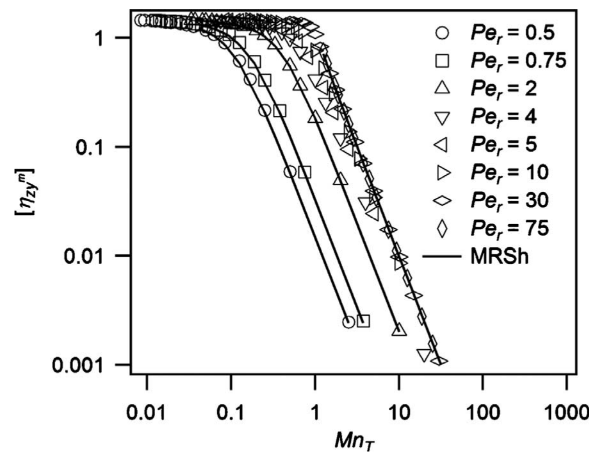

FIG. 6. Intrinsic magnetoviscosity as a function of the torque-based Mason number for various values of the dimensionless shear rate Pe_r. The solid lines correspond to the predictions of the MRSh equation for $Pe_r=0.25$, 0.75, 2, and 75, from left to right.

A critical Mason number $Mn_{T,crit}$ can be defined to characterize the transition between approximately constant intrinsic magnetoviscosity and shear thinning following power-law behavior. This is done by extrapolating the power-law region to intercept the line corresponding to $[\eta_{zy}^m] = \frac{3}{2}$, resulting in the relationship

$$\frac{3}{2} \equiv A\ Mn_{T,crit}^{-2}. \tag{30}$$

Note that this definition of $Mn_{T,crit}$ implies

$$[\eta_{zy}^m] = \frac{3}{2}\left[\frac{Mn_{T,crit}}{Mn_T}\right]^2, \tag{31}$$

in the shear thinning region, which allows us to determine the values of $Mn_{T,crit}$.

Figure 7 illustrates the Pe_r dependence of the critical Mason number $Mn_{T,crit}$. There it is seen that the critical Mason number initially increases linearly with Pe_r but eventually saturates to a value of 0.85. Interestingly, the calculated values of $Mn_{T,crit}$ follow a curve reminiscent of the Langevin function, with

$$Mn_{T,crit} \approx 0.85 L(Pe_r) = 0.85\left[\coth Pe_r - \frac{1}{Pe_r}\right]. \tag{32}$$

Combining Eq. (31) with Eq. (32) yields the as-of-yet *ad hoc* expression

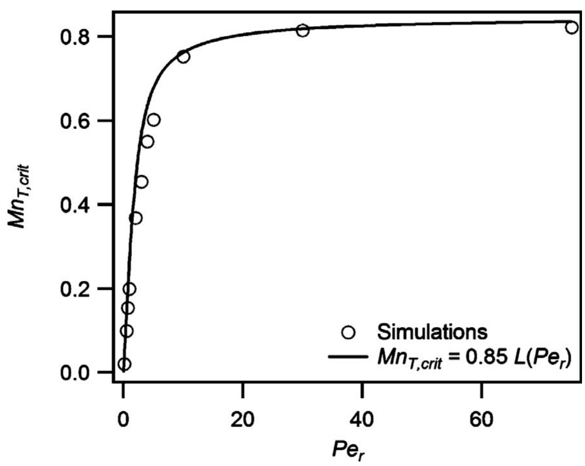

FIG. 7. Critical Mason number $\mathrm{Mn}_{T,crit}$ as a function of the applied dimensionless shear rate Pe_r. The solid line corresponds to the Langevin function with argument Pe_r, from Eq. (32).

$$[\eta_{zy}^m] \approx 2.1\left(\frac{L(\mathrm{Pe}_r)}{\mathrm{Mn}_T}\right)^2 \tag{33}$$

for the shear thinning region.

Figure 8 shows how Eq. (33) can be used to reduce all of the simulation results into a single master curve describing the magnetic field and shear rate dependences of the magnetoviscosity of dilute ferrofluids, by plotting the intrinsic magnetoviscosity as a function of $\mathrm{Mn}_T/L(\mathrm{Pe}_r)$. By combining the observation that for low Mn_T the magnetoviscosity is given by $[\eta_{zy}^m]=\frac{3}{2}$, whereas for large values of Mn_T it is given by Eq. (33) that results in the following correlation for the magnetoviscosity over the complete range of Mn_T and for all values of Pe_r in the simulations:

$$[\eta_{zy}^m] = \frac{3/2}{1+1.4\left[\frac{\mathrm{Mn}_T}{L(\mathrm{Pe}_r)}\right]^2}. \tag{34}$$

The predictions of Eq. (34) are shown as a solid line in Fig. 8, showing excellent agreement with all of the simulation results.

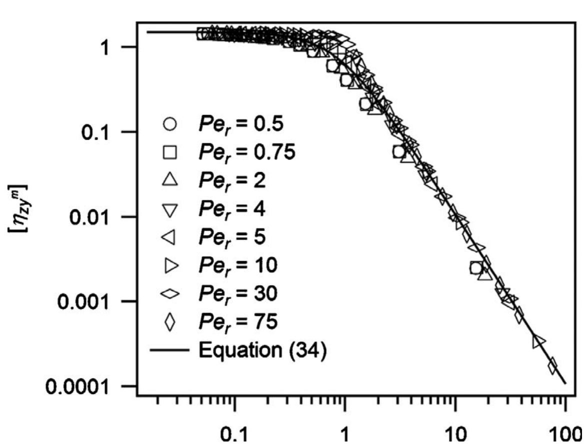

FIG. 8. Intrinsic magnetoviscosity from all simulations reduced to a single master curve using the dimensionless parameter $\mathrm{Mn}_T/L(\mathrm{Pe}_r)$. The solid line corresponds to Eq. (34).

IV. CONCLUSIONS

The rheology of dilute suspensions of spherical magnetic nanoparticles suspended in a Newtonian fluid and under applied shear and constant magnetic fields was studied through rotational Brownian dynamics simulations. For suspensions of spherical particles, excellent agreement was observed between predictions of the Martsenyuk, Raikher, and Shliomis (MRSh) relaxation equation and our direct simulations. The intrinsic magnetoviscosity calculated from Shliomis' 1972 equation deviates from the results of our simulations for intermediate values of the Langevin parameter. The use of an approximate phenomenological equation (Sh′72) for the change in magnetization results in the discrepancies observed. Similarly, the equation obtained from irreversible thermodynamics, Sh′01, presents good qualitative agreement with our results, but not quantitative agreement. Furthermore, we note that this equation incorrectly predicts the field dependence of the relaxation from equilibrium magnetization of a collection of magnetic dipoles (see the Appendix); hence, this equation cannot provide an accurate representation of the behavior of dilute ferrofluids. Our simulations also show that the assumed $\sin^2\beta$ dependence of the magnetoviscosity on the angle β between the vorticity and the magnetic field is only valid for low fields and high shear rates. Finally, it was shown that the magnetoviscosity of dilute ferrofluids can be described using a currently defined rotational Mason number given by $\mathrm{Mn}_T=\tau\dot{\gamma}/\alpha=\mathrm{Pe}_r/2\alpha$, which collapses the simulation results into a single master curve. According to this analysis, there is a critical ratio of Pe_r and α for which the suspension becomes shear thinning. This critical ratio is initially a linear function of Pe_r and then saturates for high values of Pe_r. Furthermore, in the shear thinning region the magnetoviscosity is seen to possess power-law dependence on Mn_T with an exponent of -2. Combining these observations yields a correlation for the calculated magnetoviscosity in the complete simulated Mn_T and Pe_r range with the single dimensionless parameter $\mathrm{Mn}_T/L(\mathrm{Pe}_r)$, where $L(\mathrm{Pe}_r)=\coth \mathrm{Pe}_r-1/\mathrm{Pe}_r$.

ACKNOWLEDGMENTS

This work was supported by the U.S. National Science Foundation CAREER program (Grant No. CBET-0547150) and PR-LSAMP Bridge to the Doctorate Program (Grant No. HRD-0601843).

APPENDIX: PREDICTIONS OF THE VARIOUS MAGNETIZATION RELAXATION EQUATIONS FOR THE RELAXATION FROM AN ARBITRARY EQUILIBRIUM FIELD

Differences between the magnetization relaxation equations are also manifested in their predictions for the relaxation from equilibrium magnetization in a quiescent ferrofluid after the external field is suddenly switched off. In that

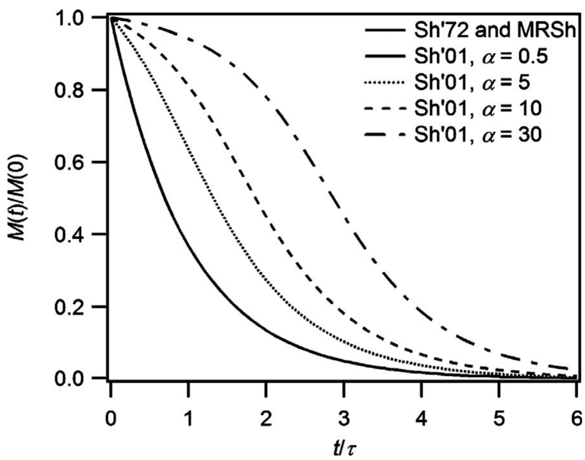

FIG. 9. Transient magnetization for an infinitely dilute ferrofluid according to the Sh′72, MRSh, and Sh′01 magnetization relaxation equations. The Sh′72 and MRSh equations both predict exponential decay regardless of the magnitude of the initial equilibrium magnetic field, whereas the Sh′01 equation only predicts exponential decay for small values of the initial equilibrium magnetic field (small values of α).

case the transient magnetization of the suspension is such that $\mathbf{\Omega}=0$ and both $\mathbf{M}$ and $\mathbf{H}_e$ are always parallel to $\mathbf{H}$. Under these conditions Eq. (4) reduces to

$$\frac{dM}{dt} = -\frac{(M - M_0)}{\tau}, \tag{A1}$$

whereas the MRSh equation (8) and the Sh′01 equation (10) reduce to

$$\frac{dM}{dt} = -\left(1 - \frac{H}{H_e}\right)\frac{M}{\tau}, \tag{A2}$$

$$\frac{dH_e}{dt} = -\frac{(H_e - H)}{\tau}, \tag{A3}$$

respectively. These equations were integrated numerically, and the predicted relaxation is shown in Fig. 9. For Eqs. (29) and (30) the decay in reduced magnetization follows an exponential behavior, while Eq. (31) only predicts exponential behavior in the limit of $\alpha \ll 1$. Direct solution of the particle orientational distribution function for the case of noninteracting particles yields exponential decay regardless of the magnitude of the initial field [40], hence indicating that the Sh′01 equation incorrectly predicts the dynamic response of dilute ferrofluids to a step decrease in the magnetic field strength.

[1] S. Odenbach, *Ferrofluids* (Springer, Berlin, 2002).
[2] S. Odenbach, *Magnetoviscous Effects in Ferrofluids* (Springer, Berlin, 2002).
[3] R. E. Rosensweig, R. Kaiser, and G. Miskolczy, J. Colloid Interface Sci. **29**, 680 (1969).
[4] J. P. McTague, J. Chem. Phys. **51**, 133 (1969).
[5] M. I. Shliomis, Sov. Phys. JETP **34**, 1291 (1972).
[6] M. I. Shliomis, Phys. Rev. E **64**, 060501 (2001).
[7] M. A. Martsenyuk, Yu L. Raikher, and M. I. Shliomis, Sov. Phys. JETP **38**, 413 (1974).
[8] B. U. Felderhof, Phys. Rev. E **62**, 3848 (2000).
[9] P. Ilg, Eur. Phys. J. E **26**, 169 (2008).
[10] H. C. Weng, C.-L. Chen, and C. K. Chen, Phys. Rev. E **78**, 056305 (2008).
[11] H. W. Müller and M. Liu, Phys. Rev. E **64**, 061405 (2001).
[12] A. O. Tsebers, Magnetohydrodynamics **20**, 343 (1984).
[13] S. Odenbach and H. Stork, J. Magn. Magn. Mater. **183**, 188 (1998).
[14] L. M. Pop *et al.*, Appl. Organomet. Chem. **18**, 523 (2004).
[15] L. Vékás *et al.*, Prog. Colloid Polym. Sci. **117**, 104 (2001).
[16] J. Vicente *et al.*, Rheol. Acta **44**, 94 (2004).
[17] R. Y. Hong *et al.*, Chem. Eng. Sci. **62**, 5912 (2007).
[18] G. Bossis *et al.*, Prog. Colloid Polym. Sci. **81**, 251 (1990).
[19] A. R. Altenberger and J. S. Dahler, J. Colloid Interface Sci. **189**, 379 (1997).
[20] N. Andhariya *et al.*, J. Colloid Interface Sci. **323**, 153 (2008).
[21] R. Patel, R. V. Upadhyay, and R. V. Mehta, J. Colloid Interface Sci. **263**, 661 (2003).
[22] A. Chaves, C. Rinaldi, S. Elborai, X. He, and M. Zahn, Phys. Rev. Lett. **96**, 194501 (2006).
[23] A. Chaves, M. Zahn, and C. Rinaldi, Phys. Fluids **20**, 053102 (2008).
[24] H. Morimoto, T. Maekawa, and Y. Matsumoto, Phys. Rev. E **65**, 061508 (2002).
[25] M. I. Shliomis and K. I. Morozov, Phys. Fluids **6**, 2855 (1994).
[26] A. Satoh and M. Ozaki, J. Colloid Interface Sci. **298**, 957 (2006).
[27] A. Satoh, J. Colloid Interface Sci. **234**, 425 (2001).
[28] J. H. Sánchez and C. Rinaldi, J. Colloid Interface Sci. **331**, 500 (2009).
[29] J. H. Sánchez and C. Rinaldi, Phys. Fluids **22**, 043304 (2010).
[30] H. Goldstein, C. Poole, and J. Safko, *Classical Mechanics* (Addison-Wesley, San Francisco, 2002).
[31] H. C. Ottinger, *Stochastic Processes in Polymeric Fluids* (Springer, Berlin, 1996).
[32] See supplementary material at http://link.aps.org/supplemental/10.1103/PhysRevE.82.046310 for calculated values of the magnetoviscosity over a range of values of the Langevin parameter and rotational Péclet number.
[33] X. He *et al.*, J. Appl. Phys. **97**, 10Q302 (2005).
[34] M. Miwa *et al.*, Tribology Lett. **15**, 97 (2003).
[35] D. J. Klingenberg, J. Rheol. **51**, 883 (2007).
[36] B.-J. d. Gans, H. Hoekstra, and J. Mellema, Faraday Discuss. **112**, 209 (1999).

[37] A. Yu Zubarev, and L. Yu Iskakova, Physica A **382**, 378 (2007).
[38] M. T. L. López-López *et al.*, Croat. Chem. Acta **80**, 445 (2007).
[39] O. G. Calderón and S. Melle, J. Phys. D: Appl. Phys. **35**, 2492 (2002).
[40] Y. P. Kalmykov and S. V. Titov, J. Chem. Phys. **126**, 174903 (2007).